Hierarchical scale curvelet interpolation of aliased seismic data

Mostafa Naghizadeh and Mauricio Sacchi

SUMMARY

We propose a robust interpolation scheme for aliased regularly sampled seismic data that uses the curvelet transform. In a first pass, the curvelet transform is used to compute the curvelet coefficients of the aliased seismic data. The aforementioned coefficients are divided into two groups of scales: alias-free and alias-contaminated scales. The alias-free curvelet coefficients are upscaled to estimate a mask function that is used to constrain the inversion of the alias-contaminated scale coefficients. The mask function is incorporated into the inversion via a minimum norm least squares algorithm that determines the curvelet coefficients of the desired alias-free data. Once the alias-free coefficients are determined, the curvelet synthesis operator is used to reconstruct seismograms at new spatial positions. Synthetic and real data examples are used to illustrate the performance of the proposed curvelet interpolation method.

INTRODUCTION

Interpolation and reconstruction of seismic data has become an important topic for the seismic data processing community. It is often the case that logistic and economic constraints dictate the spatial sampling of seismic surveys. Wave-fields are continuous; in other words, seismic energy reaches the surface of the earth everywhere in our area of study. The process of acquisition records a finite number of spatial samples of the continuous wave field generated by a finite number of sources. This leads to a regular or irregular distribution of sources and receivers. Many important techniques for removing coherent noise and imaging the earth interior have stringent sampling requirements which are often not met in real surveys. In order to avoid information losses, the data should be sampled according to the Nyquist criterion (Vermeer, 1990). When this criterion is not honored, reconstruction can be used to recover the data to a denser distribution of sources and receivers and mimic a properly sampled survey (Liu, 2004).

Methods for seismic wave field reconstruction can be classified into two categories: wave-equation based methods and signal processing methods. Wave-equation methods utilize the physics of wave propagation to reconstruct seismic volumes. In general, the idea can be summarized as follows. An operator is used to map seismic wave fields to a physical domain. Then, the modeled physical domain is transformed back to data space to obtain the data we would have acquired with an ideal experiment. It is basically a regression approach where the regressors are built based on wave equation principles (in general, approximations to kinematic ray theoretical solutions of the wave equation). The methods proposed by Ronen (1987), Bagaini and Spagnolini (1999), Stolt (2002), Trad (2003), Fomel (2003), Malcolm et al. (2005), Clapp (2006) and Leggott et al. (2007) fall under this category. These methods require the knowledge of some sort of velocity distribution in the earth's interior (migration velocities, root-mean-square velocities, stacking velocities). While reconstruction methods based on wave equation principles are very important, this paper will not investigate this category of reconstruction algorithms.

Seismic data reconstruction via signal processing approaches is an ongoing research topic in exploration seismology. During the last decade, important advances have been made in this area. Currently, signal processing reconstruction algorithms based on Fourier synthesis operators can cope with multidimensional sampling as demonstrated by several authors (Duijndam et al., 1999; Liu et al., 2004; Zwartjes and Gisolf, 2006; Schonewille et al., 2009). These methods are based on classical signal processing principles and do not require information about the subsurface. However, they utilize specific properties of seismic data as apriori information for interpolation purposes. In addition, most of these methods are quite robust in situations where the optimality condition under which they were designed are not completely satisfied (Trad, 2009).

The main contribution of this paper is the introduction of a strategy that utilizes the curvelet transform to interpolate regularly sampled aliased seismic data. It is important to stress that the curvelet transform has been used by Hennenfent and Herrmann (2007, 2008) and Herrmann and Hennenfent (2008) to interpolate seismic data. In their articles, they reported the difficulty of interpolating regularly sampled aliased data with the curvelet transform and therefore, proposed random sampling strategies to circumvent the aliasing problem. In this paper, however, we propose a new methodology which successfully eliminates the requirement of randomization to avoid aliasing. We create a mask function from the alias-free curvelet scales (low frequencies) to constrain the interpolation of alias-contaminated scales (high frequencies). The proposed method is an attempt to utilize early principles of *f-x* and *f-k* domain beyond alias interpolation methods (Spitz, 1991; Gulunay, 2003) in the curvelet domain. In summary, by carefully understanding well-established beyond alias interpolation methods (Spitz, 1991; Gulunay, 2003) in conjunction with novel signal processing tools like the curvelet transform (Candes et al., 2005), we were able to develop an algorithm capable of reconstructing aliased regularly sampled data. Alias-free (coarse) scales can drive the inversion of fine scale curvelet coefficients because we assume that the local dip of a seismic event is constant for all frequencies. In other words, we assume non-dispersive seismic events.

THEORY

The curvelet transform

The curvelet transform is a local and directional decomposition of an image (data) into harmonic scales (Candes and Donoho, 2004). The curvelet transform aims to find the contribution from each point of data in the *t-x* domain to isolated directional windows in the *f-k* domain. If we assume that $m(t,x)$ represents seismic data in the *t-x* domain, we define a set of functions $\varphi(s,\theta,t,x)$, where s indicates scale (increasing from coarsest to finest), θ, is angle or dip and t_0, x_0 are the *t-x* location parameters. These functions, known as curvelets, are used to decompose the original data in local components of various scales and dip. Curvelets can be considered as wavelets with the additional important property of directionality (dip). The continuous curvelet transform can be represented as the inner product of the data $m(t,x)$ and the curvelet function

$$c(s,\theta,t_0,x_0) = \mathscr{C}[m] = \int_t \int_x m(t,x)\,\varphi(s,\theta,t_0-t,x_0-x)\,dt\,dx\,. \quad (1)$$

In our study we will adopt the discrete curvelet transform (Candes et al., 2005). The latter is an efficient implementation of the above equation where the number of coefficients varies with scale and direction. This leads to a smaller number of curvelet coefficients in the coarser scales with respect to the finer scales. The mathematical basics of curvelets and discrete curvelet transforms are fully developed and discussed in Candes et al. (2005) and Candes and Donoho (2004). Our algorithm was developed utilizing the curvelet transform provided by the package `CurveLab`. In the rest of this article, we refer to the discrete curvelet transform as curvelet transform.

Figure 1a shows the partitioning of the *f-k* domain adopted by the curvelet transform. This example contains 6 scales represented by the co-centric squares (in this case half of the *f-k* plane since we assume real *t-x* signals/images). Except for scale 1 (coarsest scale), the rest of scales are divided into smaller windows each representing a specific direction. The coarsest scale of the curvelet transform does not have directional properties. Notice that the finest scale (scale 6 in this example) covers 75% of the *f-k* domain. For completeness, we have also indicated the 8 directions associated with scale 4. For the methodology discussed in this paper, the directional properties of the curvelets are of great importance. We will also display the curvelet coefficient as t_0-x_0 patches positioned in a large matrix according to the patch scale and nominal angle or dip. The latter is shown in 1b.

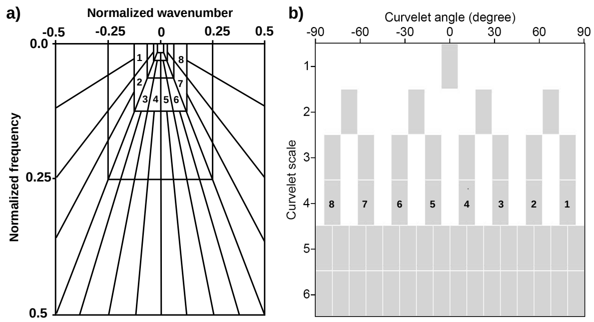

Figure 1: a) Curvelet windows in the *f-k* domain. b) Representation of the curvelet coefficients which is adopted in this article.

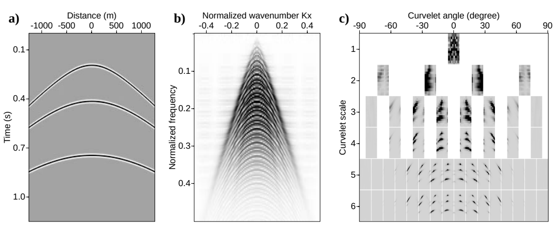

Figure 2: Synthetic seismic data. a) Data in the *t-x* domain. b) Data in the *f-k* domain. c) Data in the curvelet domain. The curvelet coefficients were scaled to patches of size 50×50 for illustration purposes.

We will use a simple example to illustrate the decomposition of seismic data by means of the curvelet transform. For this purpose, we will utilize the *t-x* data portrayed in Figure 2a. To complement the analysis, we first compute the *f-k* spectrum of the data shown in Figure 2b. The coefficients of the curvelet transform are displayed in 2c. At this point, an important comment is in order: this is not the traditional way of displaying the coefficients of the curvelet transform; because the number of coefficients at a given scale and direction is variable, each patch of coefficients for a given scale and direction was upscaled/downscaled to fit a matrix of size 50×50. In addition, each re-sampled patch was placed in a representation where the horizontal axis indicates angle or direction and, the vertical axis indicates scale. This representation allows us to make a clear analogy between the data representation in the curvelet domain and the more intuitive and classical *f-k* representation.

Using matrix notation, the curvelet transform **C** can be represented as follows

$$\mathbf{c} = \mathbf{C}\mathbf{m}, \tag{2}$$

where the discrete set of coefficients computed by the curvelet transform is represented via the vector **c**. Similarly, the *t-x* discrete data are represented by the vector **m** and the transform via the matrix **C**. One needs to stress, however, that the coefficients and the data are not stored in vector format. Moreover, the curvelet transform is not implemented via an explicit matrix multiplication. The latter is just a notation that permits us to use the simple language of linear algebra to solve our reconstruction problem.

The discrete curvelet transform is a tight frame and therefore, the adjoint operator $\mathbf{C}^T$ is equal to the pseudo-inverse of **C** (Candes and Donoho, 2004). Consequently, the inverse curvelet transform (our synthesis operator) is obtained using the adjoint transform

$$\mathbf{m} = \mathbf{C}^T\mathbf{c}. \tag{3}$$

Minimum norm least squares curvelet interpolation

We now turn our attention to the problem of reconstructing seismic data using the curvelet transform. For this purpose, we denote **m** our desired interpolated data in the *t-x* domain. In addition, the available traces are indicated by **d**. The available traces and the desired data are connected via a sampling operator **G** (Liu and Sacchi, 2004)

$$\mathbf{d} = \mathbf{G}\mathbf{m} + \mathbf{n}, \tag{4}$$

where we have also incorporated the term **n** to include additive noise. The interpolation problem given by equation 4 is an under-determined problem, therefore a priori information is needed for solving the problem. One way to solve the aforementioned problem is by introducing a change of variable and a regularization term to guarantee the stability and uniqueness of the solution. We posed the reconstruction problem in the curvelet domain (the change of variable) and, to attain this goal, we represent the data in terms of curvelet coefficients. The latter will allow us to incorporate a priori information about directionality and scale (frequency content) into our anti-alias interpolation scheme. The curvelet adjoint operator is used to represent the desired data. The alias-free desired data will be represented via

$$\mathbf{m} = \mathbf{C}^T\mathbf{W}\mathbf{c}, \tag{5}$$

where we have introduced a mask function **W** that serves to preserve the subset of alias-free curvelet coefficients. Inserting equation 5 into 4 yields

$$\mathbf{d} = \mathbf{G}\mathbf{C}^T\mathbf{W}\mathbf{c} + \mathbf{n}. \tag{6}$$

The mask function **W** is a diagonal matrix with elements that are either 0 or 1 so we are trying to prescribe with **W** the elements of the curvelet that are used to represent the desired data. Before describing how one can compute this important operator, let us assume for the moment that the operator **W** is known. The system of equations given by expression is under-determined (Menke, 1989) and therefore, it admits an infinite number of solutions. A stable and unique solution can be found by minimizing the following cost function (Tikhonov and Goncharsky, 1987)

$$J = ||\mathbf{d} - \mathbf{G}\mathbf{C}^T\mathbf{W}\mathbf{c}||_2^2 + \mu^2||\mathbf{c}||_2^2. \tag{7}$$

The minimum of the cost function J can be computed using the method of conjugate gradients (Hestenes and Stiefel, 1952). The advantage of using a semi-iterative solver like conjugate gradients is that there is no need of explicit knowledge of **C** in matrix form. The method of conjugate gradients requires the action of the operator $\mathbf{C}^T$ and **C** on a vector in the coefficient and data spaces, respectively. The latter is a feature of conjugate gradients, and in general of many iterative and semi-iterative solvers, that is fully exploited in many seismic processing and inversion problems (Claerbout, 1992). The goal of the proposed algorithm is to find the coefficients $\hat{\mathbf{c}}$ that minimize J and, use them to reconstruct the data via the curvelet adjoint operator $\hat{\mathbf{m}} = \mathbf{C}^T\hat{\mathbf{c}}$.

Selection of W for regularly decimated aliased data

This section describes a strategy to estimate **W** from the data, which is a key component of our algorithm. We first use the curvelet transform to find an initial vector of coefficients **c** (equation 2). The coefficients are divided into two groups according to their scale: alias-free and alias-contaminated scales. Let us define the indices j and l that indicate scale and angle, respectively. Furthermore, the parameter j_a indicates the index of the maximum alias-free scale. With this definition in mind, the mask function for the alias-free scales can be computed as follows

$$[\mathbf{W}]_{j,l} = \begin{cases} 0 & |[\mathbf{c}]_{j,l}| < \lambda_j \\ 1 & |[\mathbf{c}]_{j,l}| \geq \lambda_j \end{cases} \quad \texttt{if} \quad j \leq j_a, \tag{8}$$

where $[\mathbf{c}]_{j,l}$ is used to indicate all the coefficients for scale j and angle l. Similarly, $[\mathbf{W}]_{j,l}$ represents all the elements of the diagonal mask function for scale j and angle l. The parameter λ_j is a user defined threshold value for scale j.

The remaining problem is to compute the mask function for alias-contaminated scales. For this purpose, we use the following algorithm

$$[\mathbf{W}]_{j,l} = \mathscr{N}[\mathbf{W}]_{j-1,\bar{l}} \quad \texttt{if} \quad j > j_a, \tag{9}$$

where in the expression above $\mathscr{N}$ denotes the nearest neighbor operator that is needed to upscale the mask function from scale $j-1$ to j and $\bar{l}$ indicates the directionality (angle) index closest to l. In essence, we use the mask function from a lower scale (alias-free) to constrain the curvelet coefficients of higher scales that are contaminated by aliasing. The mask behaves like a local and directional all-pass operator for the coefficients that are modeling the alias-free signal. In summary, equations 8 and 9 are used to estimate the mask function that will be used in the reconstruction algorithm outlined in the preceding section.

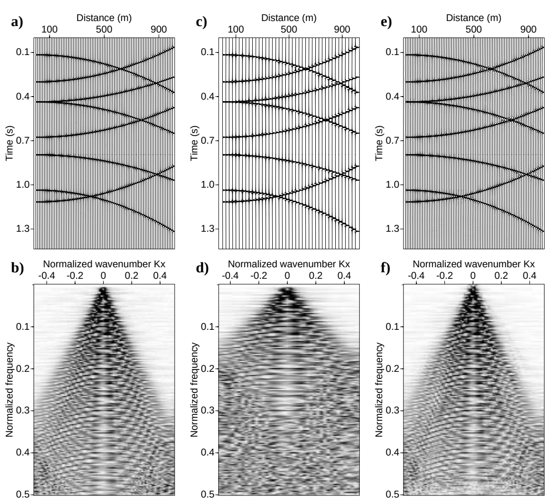

Figure 3: Synthetic data example with conflicting dips. a) Original data. c) Data after decimation by a factor of 2. c) Interpolated data. The panels b), d) and f) display the *f-k* spectra of (a), (c), and (e), respectively.

SYNTHETIC EXAMPLES

Regularly sampled aliased data with conflicting dips

To continue with the synthetic data analysis, we have created a synthetic gather that consists of 8 events with conflicting dip and variable curvature. The data and their *f-k* spectrum are portrayed in Figures 3a

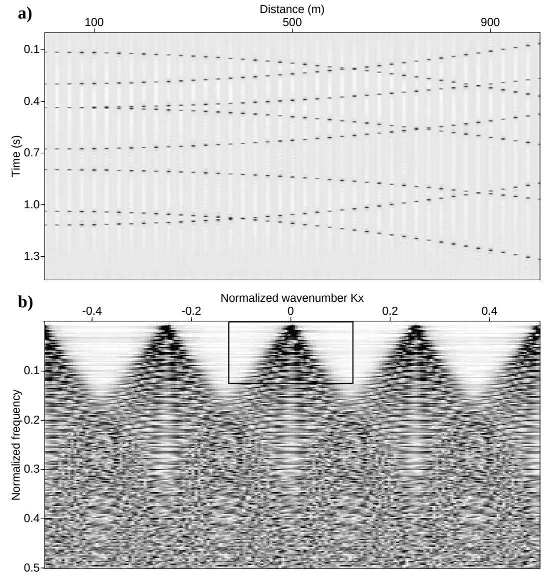

Figure 4: a) Pre-processed data for interpolation via the curvelet transform. Pre-processing is needed to guarantee that the desired signal does not have wrap-around energy in *f-k* domain. These data were obtained from Figure 3c by interlacing 4 zero traces between each pair of existing traces. This is the input to the curvelet interpolation algorithm proposed in this article. b) The *f-k* spectrum of the pre-processed data. The solid box in (b) represent the region in *f-k* where alias-free coefficients are found (scales 1-4).

and 3b, respectively. The decimated data and their *f-k* spectrum are portrayed in Figures 3c and 3d, respectively. The results of our interpolation algorithm are provided in Figures 3e and 3f. The input data to the algorithm, again, are prepared in order to secure that there is no wrap-around energy in the *f-k* domain. This is achieved by interleaving the data with zero traces (Figure 4a and b).

Figure 5a shows the curvelet panels of the input data in Figure 4a. It is easy to see that scales 1 to 4 are free of alias. On the other hand, scales 5 and 6 are heavily contaminated by aliased energy. Figure 5b shows the mask function computed from Figure 5a using Equations 8 and 9 for $j_a = 4$. Figure 5c shows the curvelet domain representation of the coefficients obtained via the minimum norm least squares method. These coefficients were used to synthesize the interpolated data portrayed in Figure 3e. Finally, the reconstruction quality for this example is given by $Q = 13.9\,\text{dB}$.

DISCUSSIONS

Curvelet coefficients have different sizes for different scales and directions. Therefore, it is not easy to provide a simple physical representation of the curvelet coefficients. In this paper, we use upscaling (or downscaling) methods to form image patches of size 50×50 samples for each individual scale and direction. This leads to an uncomplicated way of representing the curvelet transform that is amenable to seismic data processing tasks. We need to emphasize, however, that the computation of the mask function does not require us to form the 50×50 patches that we have used for visualization. The mask function is upscaled from a coarser scale to a finer scale via a simple nearest neighbor algorithm that directly operates on the curvelet coefficients at a given scale and direction. Other "tricks" could have been used to design the mask function, however, our tests indicate that our simple

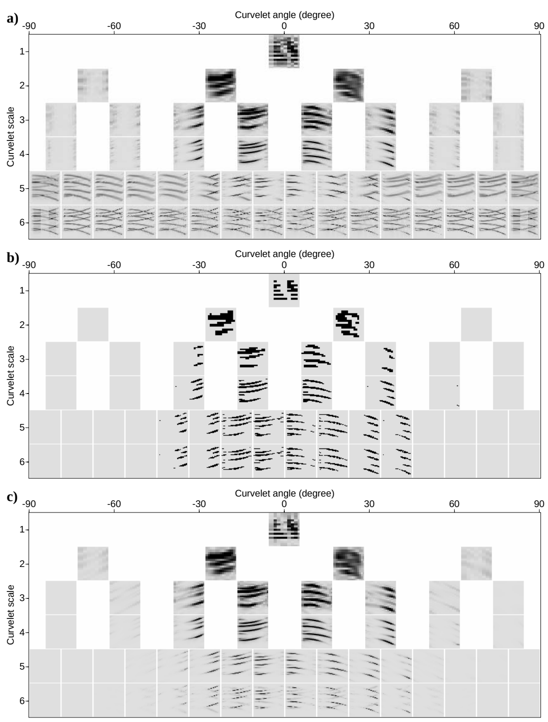

Figure 5: a) Curvelet domain representation of the data in Figure 4a. b) Mask function computed from (a) using thresholding for scales 1 to 4. The mask for scales 5-6 was bootstrapped from scale 4 using the algorithm described in the text. c) Curvelet patches of the interpolated data. The recovered data in Figure 3e were obtained by applying the adjoint curvelet operator to the inverted coefficients in (c).

nearest neighbor upscaling suffices for our needs.

We have also found that our algorithm works quite well when we set the regularization parameter $\mu = 0$ and rely on the number of iterations as an equivalent trade-off parameter. This is also often used when solving large scale linear problems (Hansen, 1987). It is also important to mention that a maximum of 10 iterations of conjugate gradients were used in all our examples. Again, the number of iterations does not seem to be a critical parameter for our interpolation scheme. The algorithm converges quite fast (approximately at 8 to 10 conjugate gradient iterations) and we have never seen any evidence of numerical instabilities.

The thresholding constant λ_j was set with the following criteria. For synthetic data, we keep 10% of the largest amplitude coefficients at a given scale. For the real data examples, we keep about 20% of the largest coefficients at a given scale. These parameters were obtained with numerical tests where we visually examined the residual data after interpolation to decide for an optimal threshold constant. When working with real data, the thresholding constant was increased because a larger number of coefficients were needed to properly model the data.

In addition, we would like to mention that existing curvelet reconstruction methods often use sparsity promoting algorithms to find a parsimonious data representation in terms of a small number of curvelet coefficients (Herrmann and Hennenfent, 2008). In this work, we have avoided sparsity-promoting algorithms and we solely relied on a minimum norm least squares algorithm implemented via the method of conjugate gradients. Finally, we stress that other methods could be used to interpolate regularly sampled aliased data with strong variation of dips. As an example we cite *f-x* adaptive interpolation (Naghizadeh and Sacchi, 2009); a fast alternative for the type of interpolation introduced here.

CONCLUSIONS

The curvelet transform is an effective tool for the decomposition of seismic data based on their local dip and frequency content. In this paper, we propose a novel method for interpolation of aliased seismic data using the curvelet transform. We have shown that spatially aliased data can be represented in the curvelet domain by two types of coefficients. Those that belong to coarser scales and that have been minimally affected by spatial sampling and those at finer scales that have been contaminated by alias. We assume that the seismic signal is expected to have similar local dips in lower and higher scales. This assumption is used to design a mask function that allows us to filter out aliased coefficients. The coefficients that survive the filtering process are fit via a minimum norm least squares algorithm that was implemented via the conjugate gradients method. The curvelet coefficients obtained via inversion are finally used to reconstruct a de-aliased version of the original data.

ACKNOWLEDGEMENTS

We thank the authors of `CurveLab [http://www.curvelet.org/]`, Emmanuel Candes, Laurent Demanet, David Donoho, and Lexing Ying for providing access to their curvelet transform codes. We acknowledge the financial support of the sponsors of the Signal Analysis and Imaging Group at the University of Alberta.

EDITED REFERENCES

Note: This reference list is a copy-edited version of the reference list submitted by the author. Reference lists for the 2010 SEG Technical Program Expanded Abstracts have been copy edited so that references provided with the online metadata for each paper will achieve a high degree of linking to cited sources that appear on the Web.

REFERENCES

Bagaini, C., and U. Spagnolini, 1999, 2-D continuation operators and their applications: Geophysics, **64**, 524–538.

Candès, E. J., L. Demanet, D. L. Donoho, and L. Ying, 2006, Fast discrete curvelet transforms: Multiscale Modeling and Simulation, **5**, no. 3, 861–899, doi:10.1137/05064182X.

Candes, E. J., and D. L. Donoho, 2004, New tight frames of curvelets and optimal representations of objects with piecewise-c2 singularities: Communications on Pure and Applied Mathematics, **57**, no. 2, 219–266.

Claerbout, J., 1992, Earth Soundings Analysis: Processing Versus Inversion: Blackwell Science.

Clapp, R. G., 2006, AMO inversion to a common azimuth dataset: SEG Expanded Abstracts, **25**, no. 1, 2097–2101, doi:10.1190/1.2369950.

Duijndam, A. J. W., M. A. Schonewille, and C. O. H. Hindriks, 1999, Reconstruction of band-limited signals, irregularly sampled along one spatial direction: Geophysics, **64**, 524–538, doi:10.1190/1.1444559.

Fomel, S., 2003, Seismic reflection data interpolation with differential offset and shot continuation: Geophysics, **68**, 733–744, doi:10.1190/1.1567243.

Gülünay, N., 2003, Seismic trace interpolation in the Fourier transform domain: Geophysics, **68**, 355–369, doi:10.1190/1.1543221.

Hansen, P. C., 1987, Rank-Deficient and Discrete Ill-Posed Problems: Numerical Aspects of Linear Inversion: Society for Industrial Mathematics.

Hennenfent, G., and F. J. Herrmann, 2007, Random sampling: New insights into the reconstruction of coarsely sampled wavefields: SEG Expanded Abstracts, **26**, 2575–2579, doi:10.1190/1.2793002.

Hennenfent, G., and F. J. Herrmann, 2008, Simply denoise: Wavefield reconstruction via jittered undersampling: Geophysics, **73**, no. 3, V19–V28, doi:10.1190/1.2841038.

Herrmann, F. J., and G. Hennenfent, 2008, Non-parametric seismic data recovery with curvelet frames: Geophysical Journal International, **173**, no. 1, 233–248, doi:10.1111/j.1365-246X.2007.03698.x.

Hestenes, M. R., and E. Stiefel, 1952, Methods of conjugate gradients for solving linear systems: Journal of Research of the National Bureau of Standards, **49**, 409–436.

Leggott, R. J., R. Wombell, G. Conroy, T. Noss, and G. Williams, 2007, An efficient leasts-quares migration: 69th EAGE Conference and Exhibition, Expanded Abstracts, P178.

Liu, B., 2004, Multi-dimensional reconstruction of seismic data: PhD thesis, University of Alberta.

Liu, B., and M. D. Sacchi, 2004, Minimum weighted norm interpolation of seismic records: Geophysics, **69**, 1560–1568, doi:10.1190/1.1836829.

Liu, B., M. D. Sacchi, and D. Trad, 2004, Simultaneous interpolation of 4 spatial dimensions: SEG Expanded Abstracts, **23**, no. 1, 2009–2012, doi:10.1190/1.1851187.

Malcolm, A. E., M. V. de Hoop, and J. H. LeRousseau, 2005, The applicability of dip moveout/azimuth moveout in the presence of caustics: Geophysics, **70**, no. 1, S1–S17, doi:10.1190/1.1852785.

Marple, S. L., ed., 1987, Digital spectral analysis with applications: Prentice-Hall Inc.

Menke, W., 1989, Geophysical Data Analysis: Discrete Inverse Theory: Academic Press.

Naghizadeh, M., and M. D. Sacchi, 2007, Multi-step auto-regressive reconstruction of seismic records: Geophysics, **72**, no. 6, V111–V118, doi:10.1190/1.2771685.

Naghizadeh, M., and M. D. Sacchi, 2009, f-x adaptive seismic-trace interpolation: Geophysics, **74**, no. 1, V9–V16, doi:10.1190/1.3008547.

Ronen, J., 1987, Wave-equation trace interpolation: Geophysics, **52**, 973–984, doi:10.1190/1.1442366.

Schonewille, M., A. Klaedtke, A. Vigner, J. Brittan, and T. Martin, 2009, Seismic data regularization with the anti-alias anti-leakage Fourier transform: First Break, **27**, 85–92.

Spitz, S., 1991, Seismic trace interpolation in the F-X domain: Geophysics, **56**, 785–794, doi:10.1190/1.1443096.

Stolt, R. H., 2002, Seismic data mapping and reconstruction: Geophysics, **67**, 890–908, doi:10.1190/1.1484532.

Tikhonov, A. N. and A. V. Goncharsky, 1987, Ill-posed problems in the natural sciences: MIR Publisher.

Trad, D., 2003, Interpolation and multiple attenuation with migration operators: Geophysics, **68**, 2043–2054, doi:10.1190/1.1635058.

Trad, D., 2009, Five-dimensional interpolation: Recovering from acquisition constraints: Geophysics, **74**, no. 6, V123–V132, doi:10.1190/1.3245216.

Vermeer, G., 1990, Seismic wavefield sampling, volume 4: Society of Exploration Geophysicists.

Zwartjes, P., and A. Gisolf, 2006, Fourier reconstruction of marinestreamer data in four spatial coordinates: Geophysics, **71**, no. 6, V171–V186, doi:10.1190/1.2348633.